FILE COPY

674

SUMMARY REPORT ON THE SECOND WIND TUNNEL TEST OF THE BOEING LFC MODEL

(NASA-CR-157792) SUMMARY REPORT OF THE SECOND WIND TUNNEL TEST OF THE BOEING LFC MODEL (Boeing Commercial Airplane Co., Seattle) 27 p HC A03/MF A01 CSCL 01A
N79-17799
Unclas
G3/02 15314

CONTRACT NAS1-14630

July 26, 1978

BOEING COMMERCIAL AIRPLANE COMPANY
P. O. Box 3707
Seattle, Washington 98124

32295

SUMMARY REPORT ON THE
SECOND WIND TUNNEL TEST
OF THE BOEING LFC MODEL

CONTRACT NAS1-14630

Prepared by: D. George-Falvy

INTRODUCTION

This report summarizes the preliminary results of the second wind tunnel test of the Boeing LFC model under contract NAS1-14630. The test was conducted in the 5' X 8' Boeing Research Wind Tunnel (BRWT) between May 8 and June 16, 1978. The principal objectives of the test were to explore the sensitivity of laminar flow to various forms of disturbances such as surface imperfections, contamination, off-design pressure distributions (increased crossflow) and imposed noise. The information obtained from the test results was intended to aid the development of design criteria for LFC airplanes regarding manufacturing tolerances and operational limitations.

The test program was carried out according to the plans described in reference 1. It consisted of the following four phases:

Phase I	Installation, checkout and acquisition of baseline data.
Phase II	Testing the sensitivity of LFC to surface imperfections.

Phase III — Testing the sensitivity of LFC to off-design flow conditions.

Phase IV — Surveying the acoustic environment of the model and testing the sensitivity of LFC to imposed noise.

The actual test sequence, however, deviated somewhat from the above list, inasmuch as Phase IV preceded Phase III; furthermore there was a five day suspension of the test during the week of June 5-9, 1978 because of the second oral review at Langley. During that time, however, a turbulence survey was carried out in the BRWT test section with the LFC model installed as a part of the company-funded wind tunnel calibration and development program.

This report contains a brief description of the test apparatus and model configurations as well as a summary of the preliminary results. The detailed analysis of the data is still in progress and the results of this work will be included in the final report. Since Phase IV of the test was handled by the Acoustics Staff and reported separately, no further discussion of this work is included here.

MODEL DESCRIPTION

The model, designated as TR-1370M-6, is an 8-foot span, 20-foot chord, 30° swept wing section having provisions for LFC over the first 30% of the upper surface and the first 15% of the lower surface. The model and associated test apparatus was essentially the same as during the previous test (Reference 2 provides a detailed description.) The surface imperfections were simulated by spanwise strips of self-adhesive tape or spanwise rows of discs punched out from self-adhesive tape. The height, width (or diameter) and location of the disturbances were varied. The geometric details of the various configurations are presented in Figures 1 and 2. In most cases the protuberances were placed midway between two neighboring slots, but in a few cases they were deliberately located adjacent to a slot either upstream or downstream. Also, both types were tried on the very leading edge with the intent of simulating certain features of leading edge cleaning devices.

Off-design pressure distributions were simulated by changing the model incidence angle and flap deflection. Since the incidence change required the removal, adjustment and reinstallation of parts of the wall fairings; thus being quite laborious, only one change was made. However, changing the flap deflection angle was simple and convenient.

INSTRUMENTATION

Apart from some minor refinements or additions, the instrumentation system was essentially the same as during the previous test (see reference 1). The refinements included the following:

- Two hot-film type boundary layer sensors and eight raised pitot-static type sensors were used to monitor the state of the boundary layer on the model upper surface in comparison to one hot-film probe and six raised pitot-static probes, respectively, used during the previous test.

- Provisions were made to record the indication (RMS output) of the hot film probes via an X-Y plotter. (The original setup provided only a visual display of the signal by a cathode ray tube.)

- The manometer board was set up to provide a continuous real time display of the most critical pressures measured at various points of the model, such as external and internal static pressures, flow meter indications and transition monitoring by the raised pitots.

- There was a hot-wire probe installed in one of the suction airflow ducts between the model and the orifice plate flow meter to find out whether or not the flow meter produced any flow oscillations in the suction system.

Figure 3 shows the arrangement of the model instrumentation including the boundary layer sensors and the internal and external pressure measuring parts.

SUMMARY OF TEST RESULTS

Phase I

o The baseline copnfiguration with an incidence of $\alpha = 0.5^{o}$ and incremental flap deflection of $\beta = -4^{o}/-1^{o}/+2^{o}$ (top/center/bottom) closely reproduced the nominal test condition of the previous entry. Laminar flow over the controlled area was achieved without much difficulty. Some fine tuning of the slot-flow control valves resulted in a smoother suction distribution than achieved during the previous test. Figure 4 illustrates the pressure distributions and suction flow characteristics (C_q and R_s) for the baseline configuration.

o A simple and very repeatable indicator of the suction flow rate was the pressure differential in the manifold chamber. This pressure could be read directly from a digital voltmeter and was used for establishing repeat conditions. The suction manifold pressure (ΔP_M) required for laminarization of the slotted area, increased with the tunnel dynamic pressure (q); the non-dimensional suction flow rate ($\dot{C_Q}$) however, remained essentially constant as demonstrated by Figure 5.

o From the indication of the hot-wire probe in the suction airflow duct it was concluded that no flow oscillation produced by the orifice plate was feeding through. If the orifice plate induced such oscillations at all, those were apparently damped out by the flow homogenizer, inserted between the flow meter and the model.

Phase II

The principal observations regarding the effects of surface imperfections are as follows:

- The ridge type surface protuberances were in general tolerable up to about k = 0.005 to 0.007 inches height except in regions where the crossflow was relatively high. (See figure 6)

- In certain cases even k = 0.01 was tolerable, particularly at lower tunnel speeds (Reynolds number), but this was more of an exception than a standard.

- The disk type protuberances apparently caused a more severe disturbance to LFC than the ridges as the tolerable protrusion heights were lower. (See figure 7)

- The tolerable protrusion height for both types of roughness elements was not significantly affected by suction flow rate. In other words, the model was able to tolerate a certain disturbance at the suction rate established for the clean condition but the limit of tolerance could not be increased noticeably by added suction.

- The sensitivity to oversuction, in fact, became more pronounced as the critical protrusion height was approached. In the case of the smooth model or with protuberances below the critical height, the laminar flow on the model was not affected by increased flow rate, but when the protuberances approached the critical height, oversuction could upset

LFC. This observation is well illustrated in Figure 8 by the typical indication of the hot-film turbulence sensor plotted as a function of suction manifold pressure, ΔP_M, which is analogous to C_Q for constant q.

- Another observation of significant practical consequence was that relatively large (k = 0.005 inches) surface protuberances (both ridge and the disk type) could be tolerated on the very leading edge along the stagnation line. This could be a useful feature if leading edge washing nozzles were to be installed for protection against insects.

- On the other hand, the model showed increased sensitivity to surface protuberances within the region extending from just downstream of the leading edge to about s/c = 8% to 10% location. This is the region where the crossflow due to sweep is most noticeable.

- It was also observed that the location of the disturbance relative to the adjoining slots could also be critical. A given ridge, for example, which was tolerable when placed midway between two slots, became intolerable close to an adjacent slot (≈ .10"), be it either ahead of it or aft of it. It must be noted, however, that the suction distribution during this set of test runs was not changed and it well may be that added suction applied locally right after the disturbance might have been effective in keeping the flow laminar downstream of the disturbance.

- One of the tasks of the data analysis is to evaluate the so-called critical roughness Reynolds nubers that represent the limiting values of permissible surface imperfections expressed in generalized terms. The Reynolds number based on protrusion height is expressed as

$$R_k = \frac{U_k k}{\nu}$$

where k is the height of the protrusion and U_k is the local velocity within the boundary layer at a height of $y = k$. For convenient numerical evaluation the above relation is transcribed as

$$R_k = R_1 \sqrt{1-C_p} \left(U_k/U_e\right) \frac{k}{12}$$

where R_1 is the unit Reynolds number, C_p is the local pressure coefficient and U_k/U_e is the velocity ratio in the boundary layer at $y = k$.

Appropriate values of U_k/U_e were determined from theoretical calculations of the boundary layer profiles on the model using the experimental values of C_p and suction as required for laminarization.

Evaluation of the applicable critical roughness Reynolds numbers is still in progress but some preliminary results are included here. Figure 9 shows, for example, how the $R_{k_{crit}}$ was estimated for a typical set of data.

o A comparison of the test data processed so far with the previous results on critical roughness Reynolds numbers indicate that the present results, in general, are consistent with the previous ones in regions where the crossflow is weak. But, in regions of pronounced crossflow, apparently lower R_k limits apply. Figure 10 illustrates some of these observations.

o The test results also tend to indicate that there is no unique value of critical Reynolds number based on protrusion height, $R_k = \frac{U_k k}{\nu}$, that is attributable to a given type of disturbance (such as the height to diameter ratio of a disk, k/d) as stipulated in the literature. The tolerable disturbance height Reynolds number, in fact, appears to be strongly dependent upon the location of the disturbance and not only on its shape. This implies that the previous history (i.e. stability characteristics) of the boundary layer ahead of a disturbance has also a decisive role in determining the tolerable limits. Figure 11 illustrates this, showing the typical variation of the critical roughness Reynolds number along the test surface for a given type of surface protuberance.

Phase III

o The schedule permitted only one angle of incidence change and four flap angle variations. The intent was to simulate a low C_L off-design condition with extended favorable pressure gradient but correspondingly increased crossflow. Based on the results of the initial calibration of the model it was estimated that an incidence change of $\Delta\alpha = -0.5$ degrees would produce the desired pressure distribution. The test, however, showed that the above incidence change was not quite adequate, particularly without changing the wall fairings. An additional incidence change, however, was not attempted because of schedule limitations. Changing the flap deflection, which could be easily accomplished, was effective in shifting the C_p levels, but did not change the shape of the pressure distribution. Figure 12 shows the C_p distributions obtained with variations in angle of incidence and flap deflection.

- Laminarization of the upper surface (back to 30% chord) required somewhat lower suction airflow (C_Q) at the off-design conditions than at the baseline condition. This can be explained by the lower C_p levels and reduced adverse pressure gradient.

- In this series of experiments, the tuning of the suction system deliberately was not changed in order to see the effects of variations in the external pressure distribution on the suction flow characteristics once the system has been tuned for a given baseline condition. (An LFC airplane would probably have to deal with a similar situation.) The results indicated that changing external pressure distributions did alter the suction inflow distributions and certain portions of the model did receive more than adequate suction while others received only a marginally adequate amount. Figure 13 illustrates this showing the distribution of the suction pressure differential, ΔP_s, and corresponding suction flow coefficients, C_q, for a typical off-design condition in comparison with the baseline condition. It can be seen that the area around s/c = .05 has only marginal suction, while ahead and aft of that region the suction is probably excessive.

REFERENCES

1. SUMMARY TEST PLAN: Second LFC Wind Tunnel Test Under NASA Contract NAS1-14630, April, 1978.

2. INITIAL TESTS ON A 20FT CHORD, 30° SWEPT WING SECTION WITH LAMINAR FLOW CONTROL OVER 30% OF THE CHORD, Boeing Document D6-46302, February 24, 1978 D. George-Falvy.

LIST OF FIGURES

SURFACE PROTUBERANCE CONFIGURATIONS TESTED

a) Spanwise Ridges

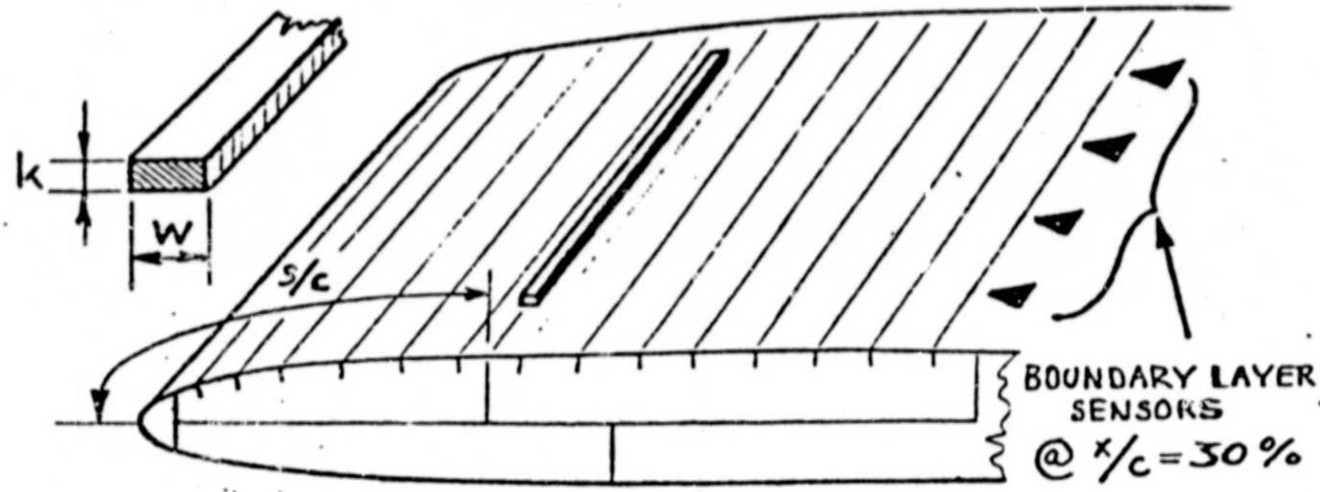

DESIGNATION	k in	W in	S/c	W/k	REMARKS
RIDGE # 1	.005	.03	.25	6.	RUN 18-24
# 2	↓	↓	.147	↓	RUN 25
# 3			.065		RUN 26
# 4			.028		RUN 27-29
# 5	↓		.016	↓	RUN 30
# 6	.010		.016	3.	RUN 31-32
# 7	↓		.10	↓	RUN 33-35
# 8	↓		.26	↓	RUN 36-39
# 9	.005	↓	.0125	6.	RUN 40 ; .05" AFT OF 1st SLOT
# 16	.005	.12	.016	24.	RUN 101-102
# 17	↓	↓	.020	↓	RUN 103 ; .05" AHEAD OF 2nd SLOT
# 18			.021		RUN 104-105 ; .05" AFT OF 2nd SLOT
# 19			.0125		RUN 106-107 ; .05" AFT OF 1st SLOT
# 20			0		RUN 108-112 LEADING E.
# 21	↓	↓	.0075	↓	RUN 113 1" AHEAD OF 1st SLOT

ORIGINAL PAGE IS OF POOR QUALITY

FIG. 1

SURFACE PROTUBERANCE CONFIGURATIONS TESTED

b) Spanwise Rows of Disks

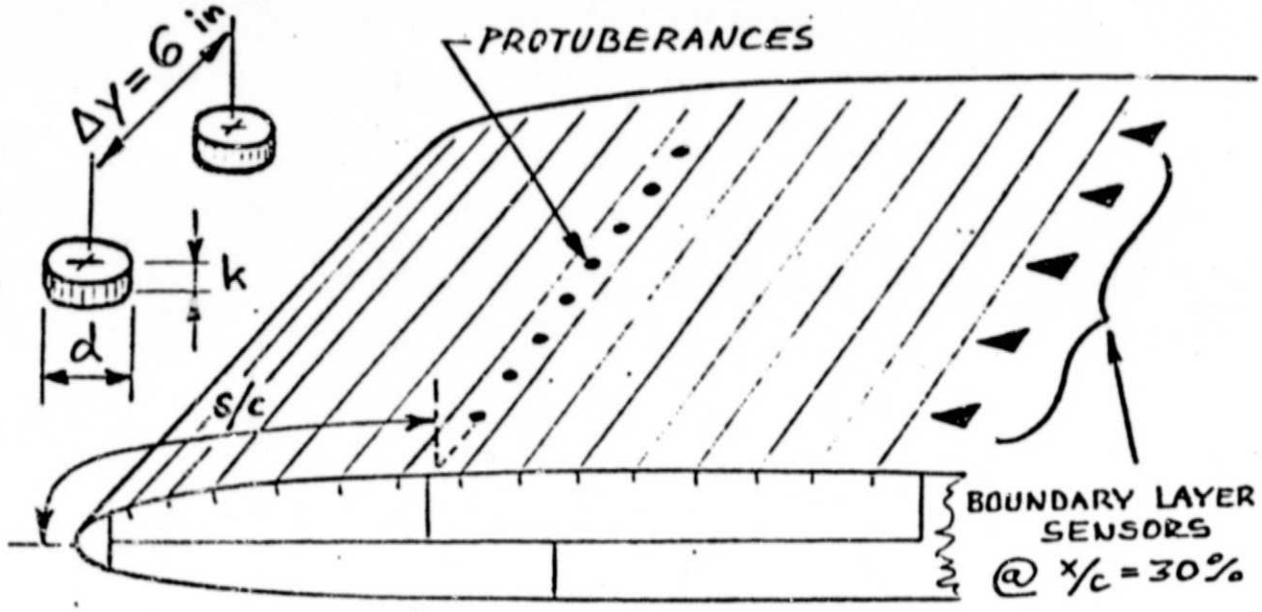

DESIGNATION	k in	d in	s/c	d/k	REMARK
DISK # 10	.01	.04	.21	4.	RUN 42-50
# 11	.005			8.	RUN 52-66
# 12	.0075			5.3	RUN 67-73
# 13	.006		.14	6.6	RUN 74-90
# 14	.005	.10	.065	20.	RUN 98-99
# 15	.005	.06		12.	RUN 100
# 22	.002	.10		50.	RUN 114-115
# 23	.004			25.	RUN 116
# 24	.002		.016	50.	RUN 117
# 25			.029	50.	RUN 118-119
# 26	.004		0	25	RUN 120; LEADING EDGE

FIG. 2

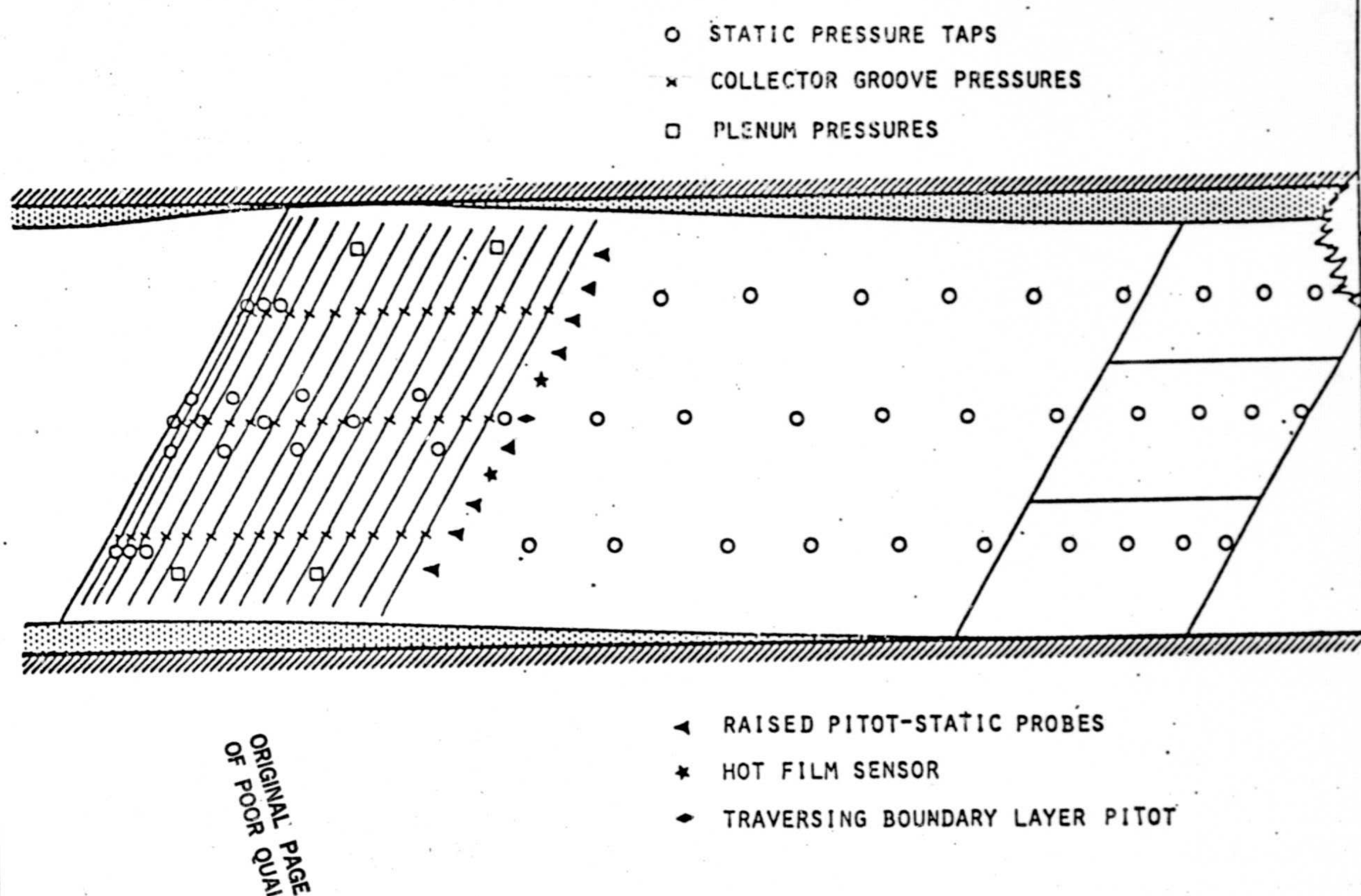

FIG. 3 INSTRUMENTATION OF THE MODEL

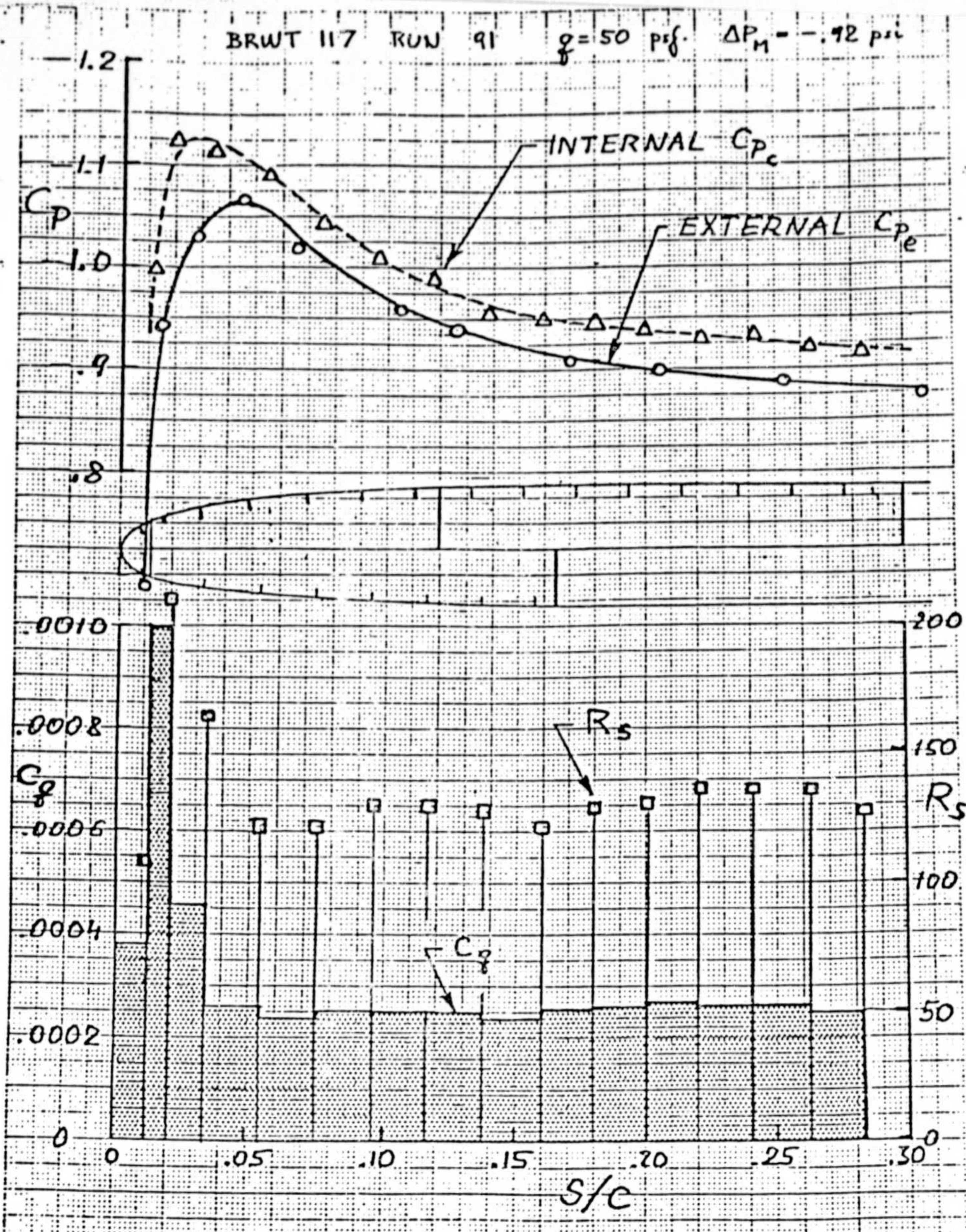

CALC		REVISED	DATE
CHECK	George Faly		
APR			
APR			

BASELINE PRESSURE DISTRIBUTIONS AND SUCTION FLOW CHARACTERISTICS

FIG. 4

PAGE

THE BOEING COMPANY

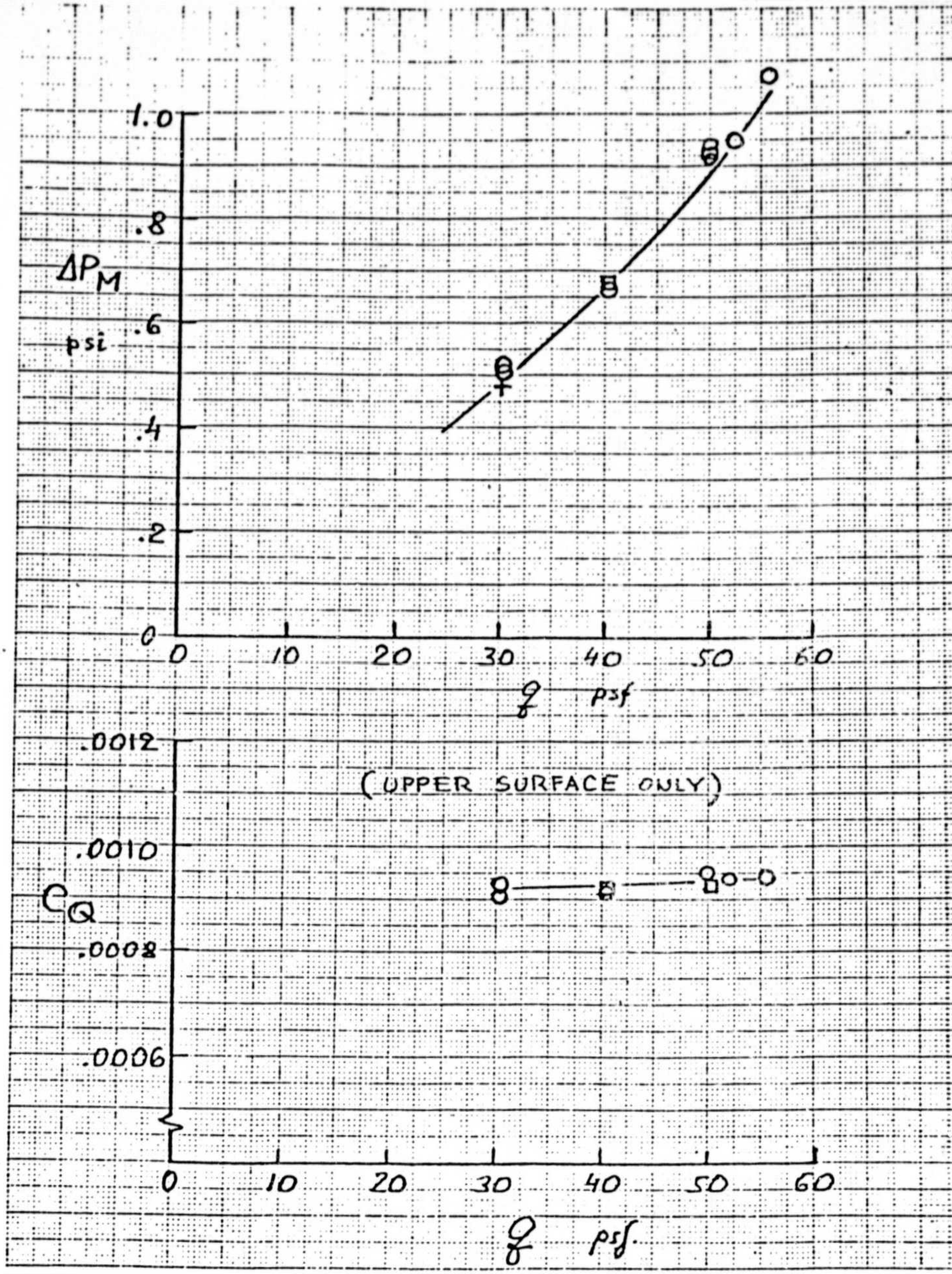

		REVISED	DATE	
CALC				SUCTION MANIFOLD PRESSURE AND FLOW COEFFICIENT REQUIRED FOR THE BASELINE CONFIGURATION
CHECK	George Falvy			
APR				
APR				
				THE BOEING COMPANY

PAGE
FIG. 3

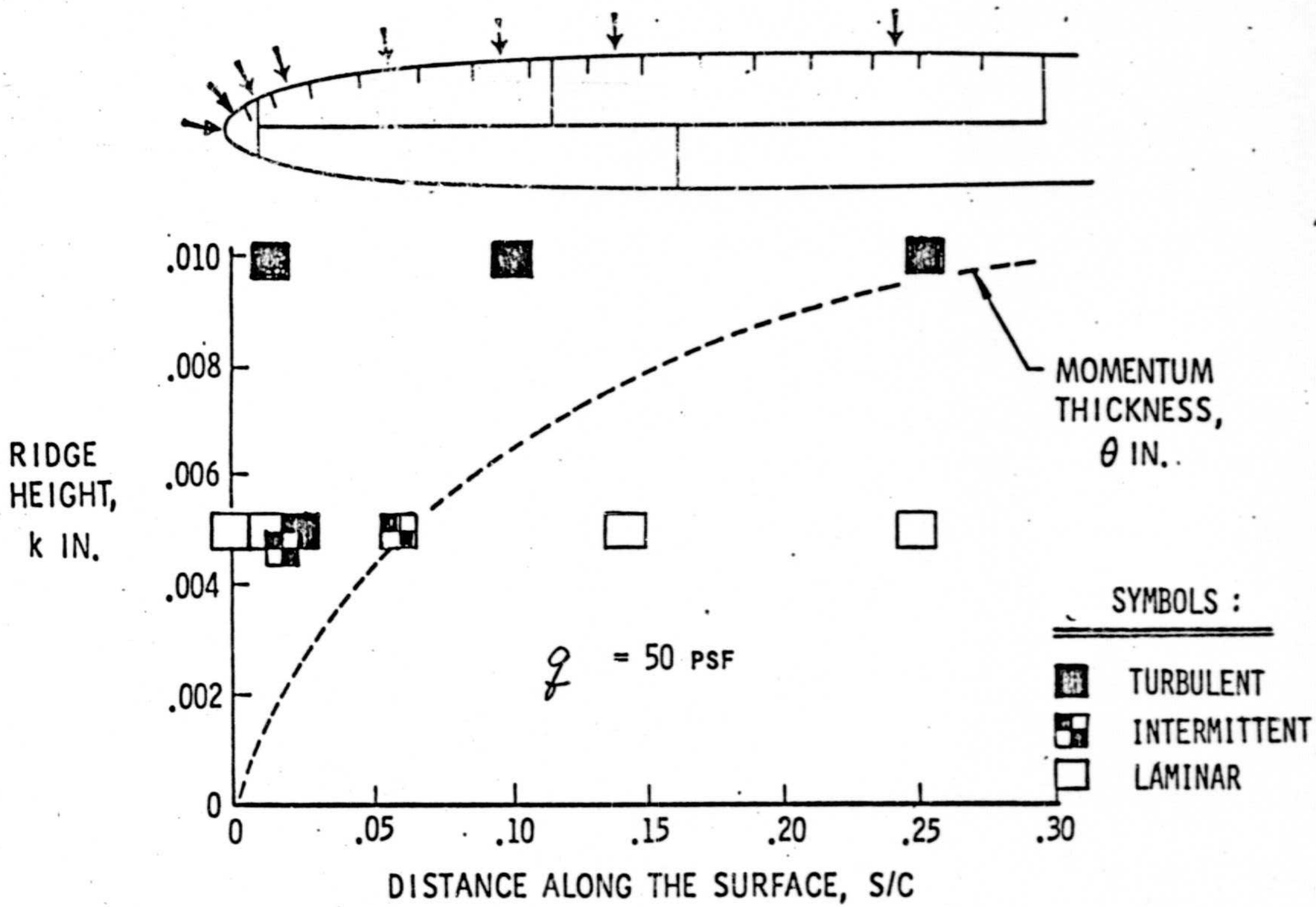

FIG. 6 TYPICAL RESULTS WITH SPANWISE RIDGES

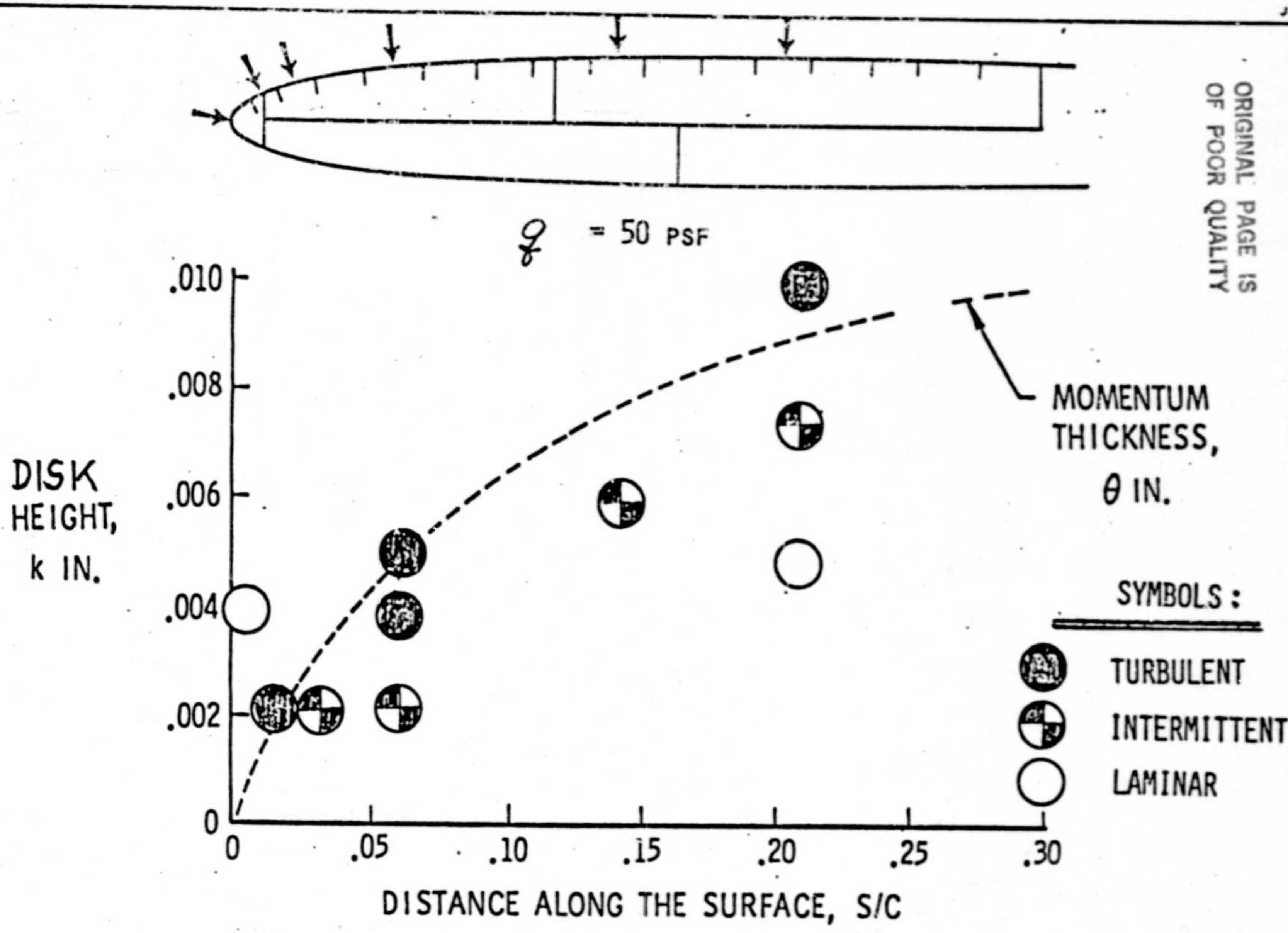

FIG. 7 TYPICAL RESULTS WITH SPANWISE ROWS OF DISCS

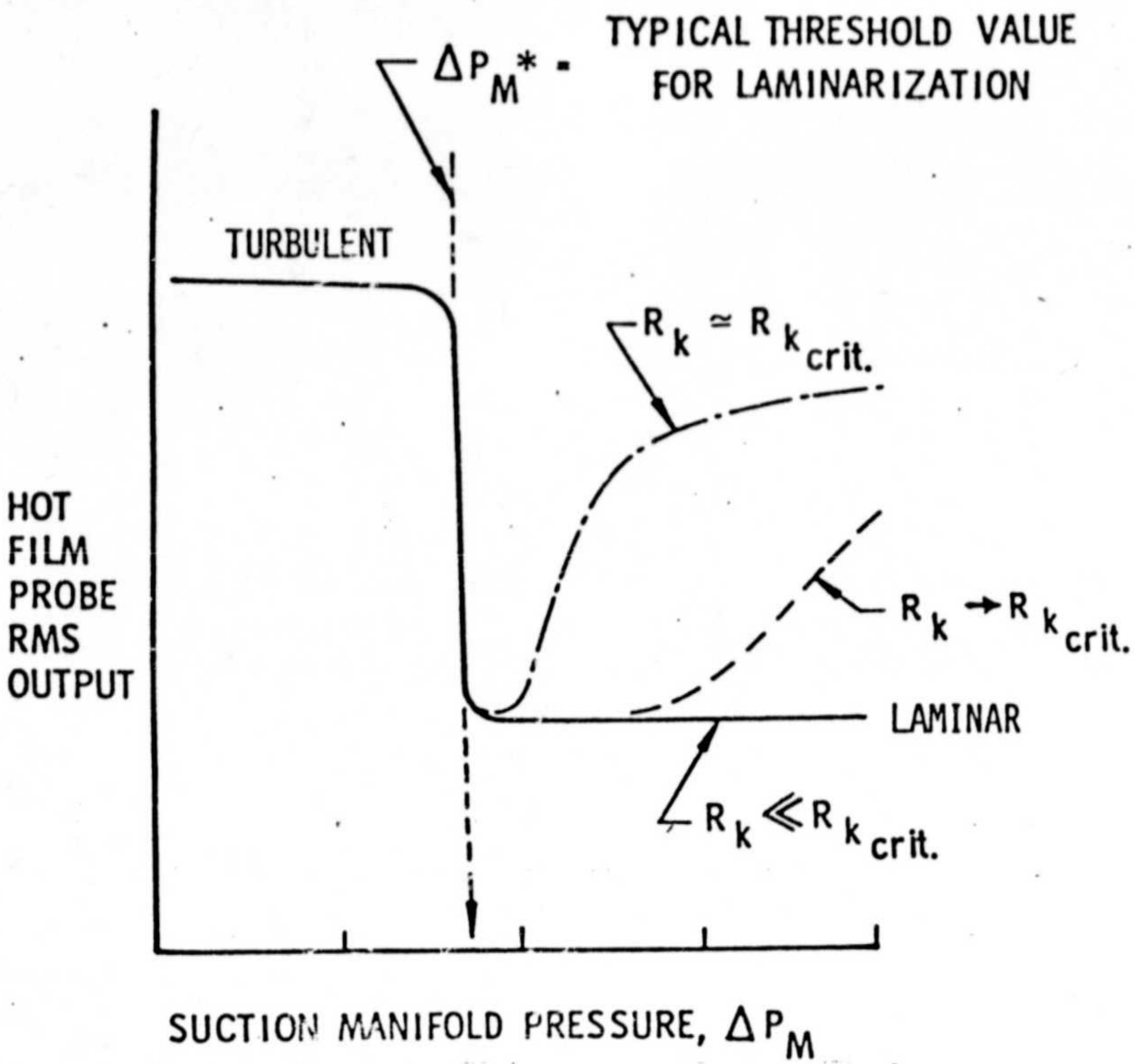

FIG. 8 EFFECT OF ROUGHNESS ON SENSITIVITY TO OVERSUCTION

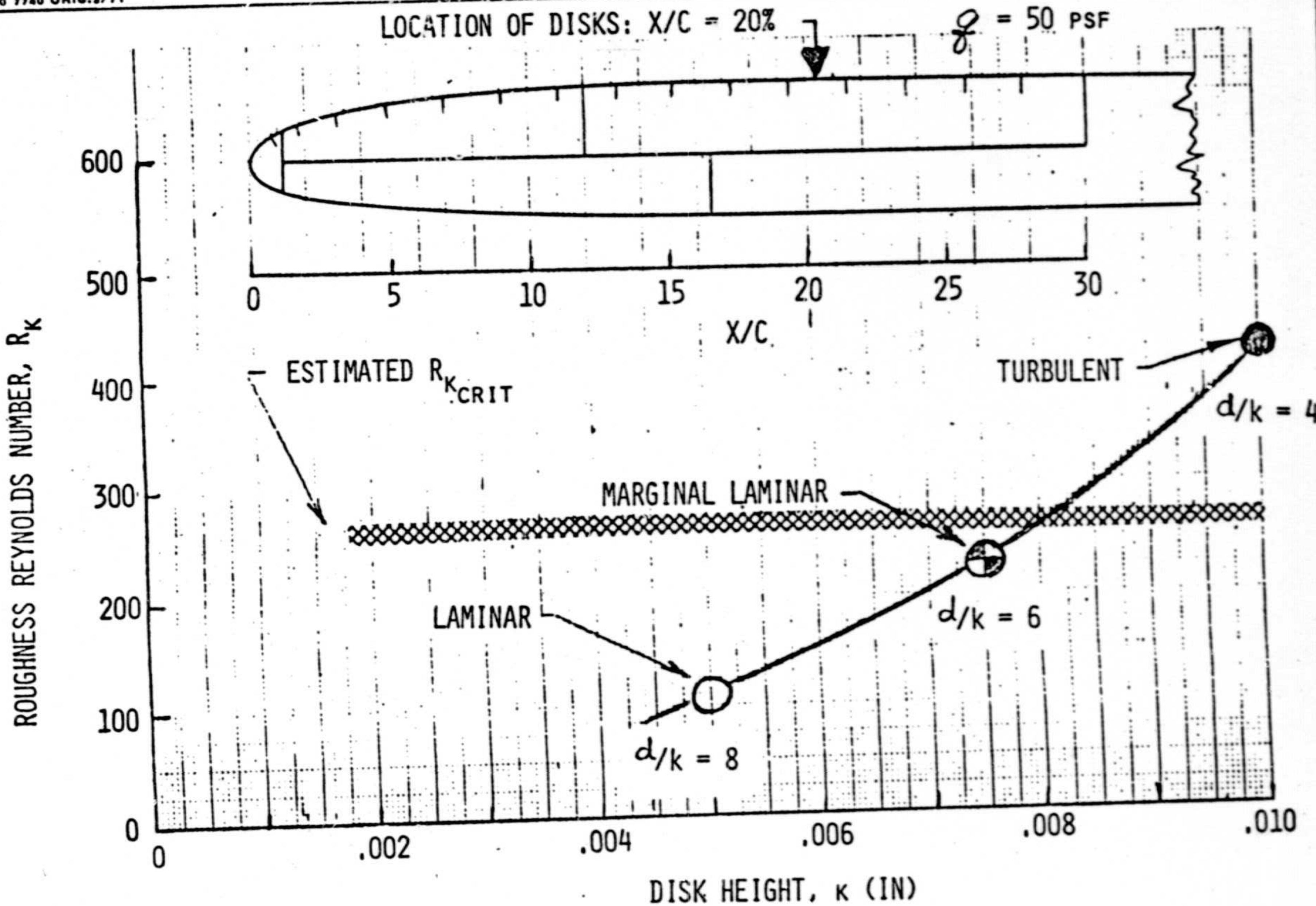

FIG. 9 DETERMINATION OF CRITICAL ROUGHNESS REYNOLDS NO. FOR A TYPICAL SET OF DISKS

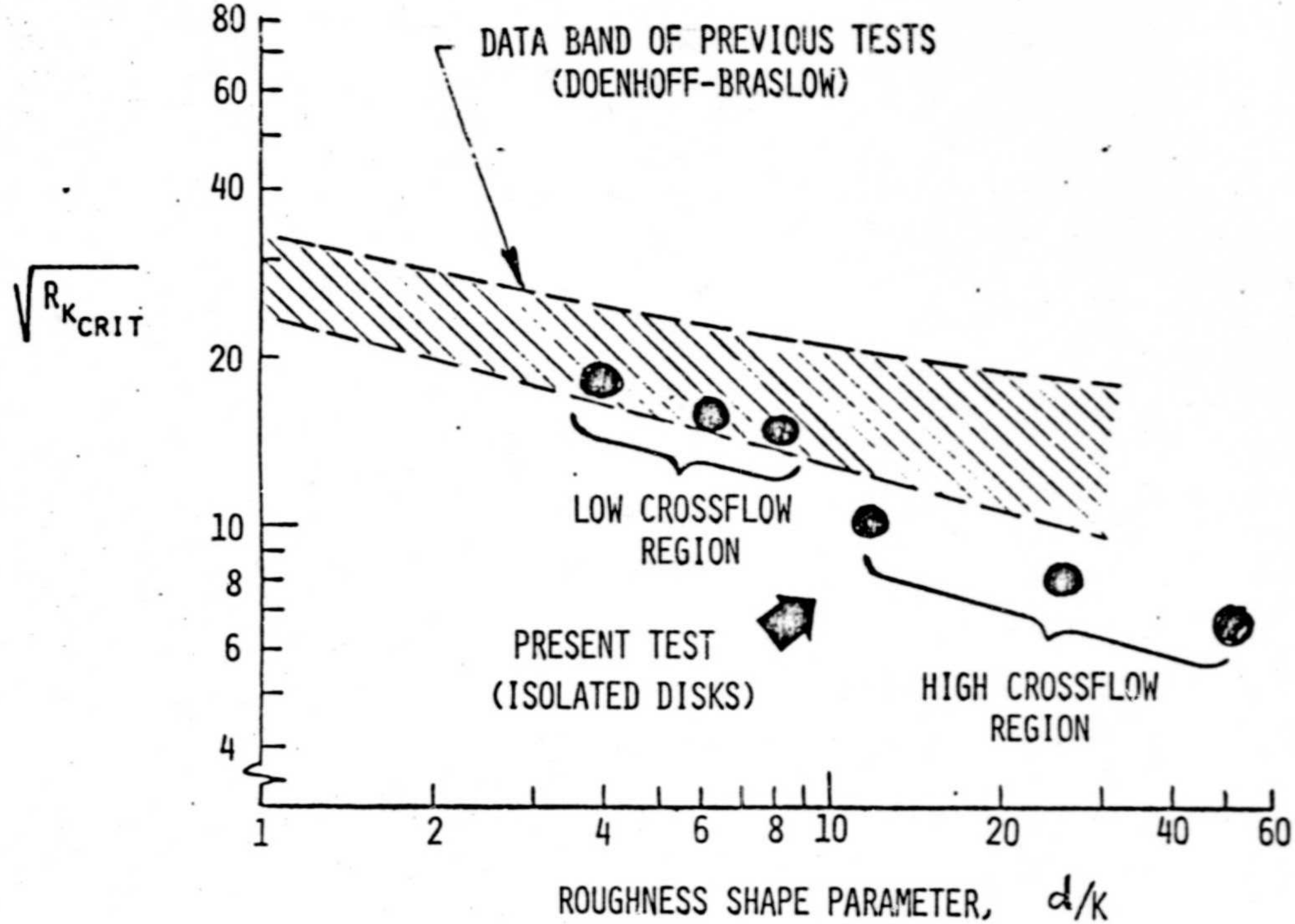

FIG. 10 COMPARISON OF PRESENT DATA ON CRITICAL ROUGHNESS REYNOLDS NUMBER WITH PREVIOUS RESULTS

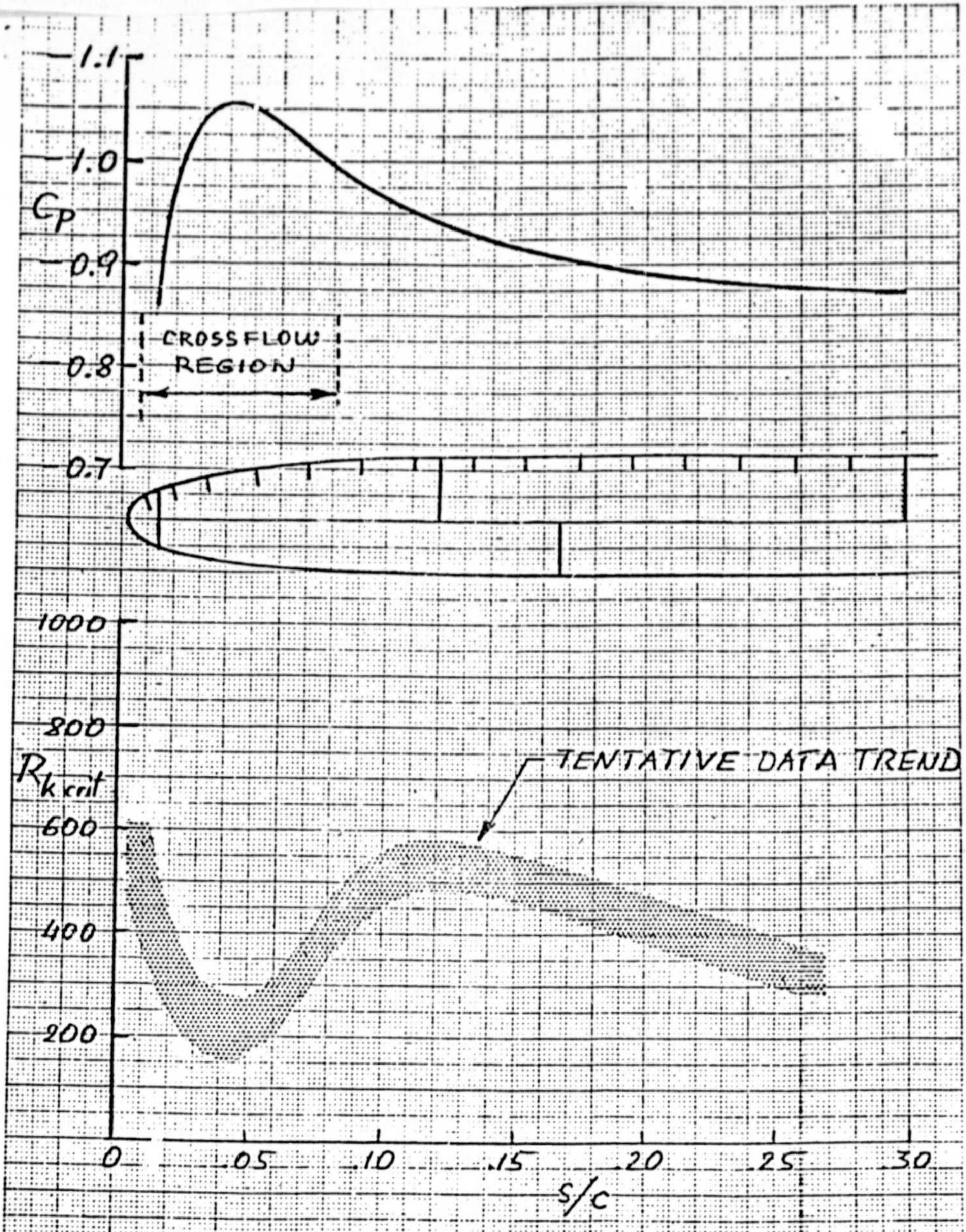

CALC	George Falvey	REVISED	DATE	CRITICAL ROUGHNESS REYNOLDS NO. AS A FUNCTION OF LOCATION
CHECK				
APR				
APR				THE BOEING COMPANY
				PAGE FIG. 11

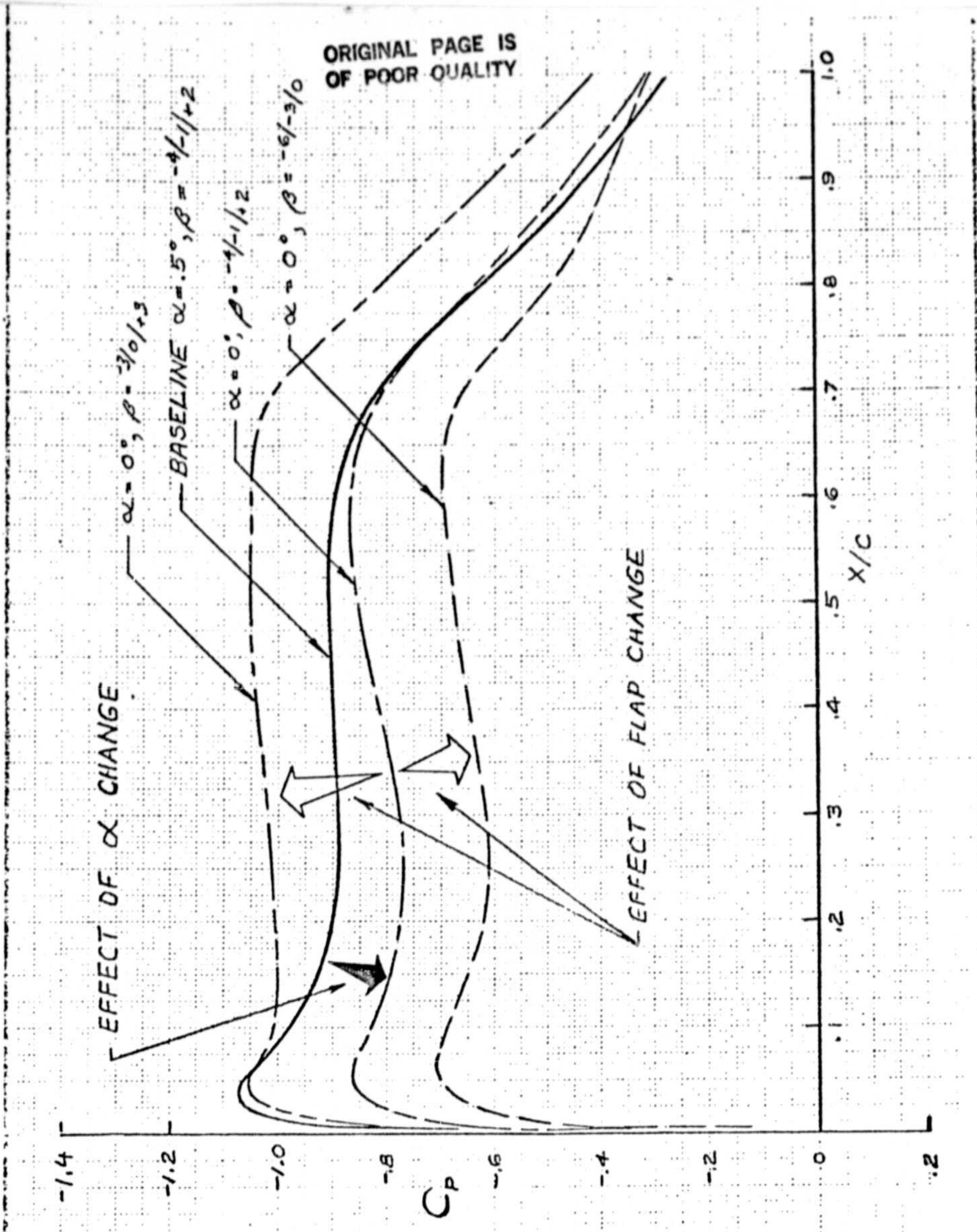

L. WRIGHT 7/28/78	OFF DESIGN PRESSURE DISTRIBUTIONS TESTED	FIG. 12
George Faley		
		25

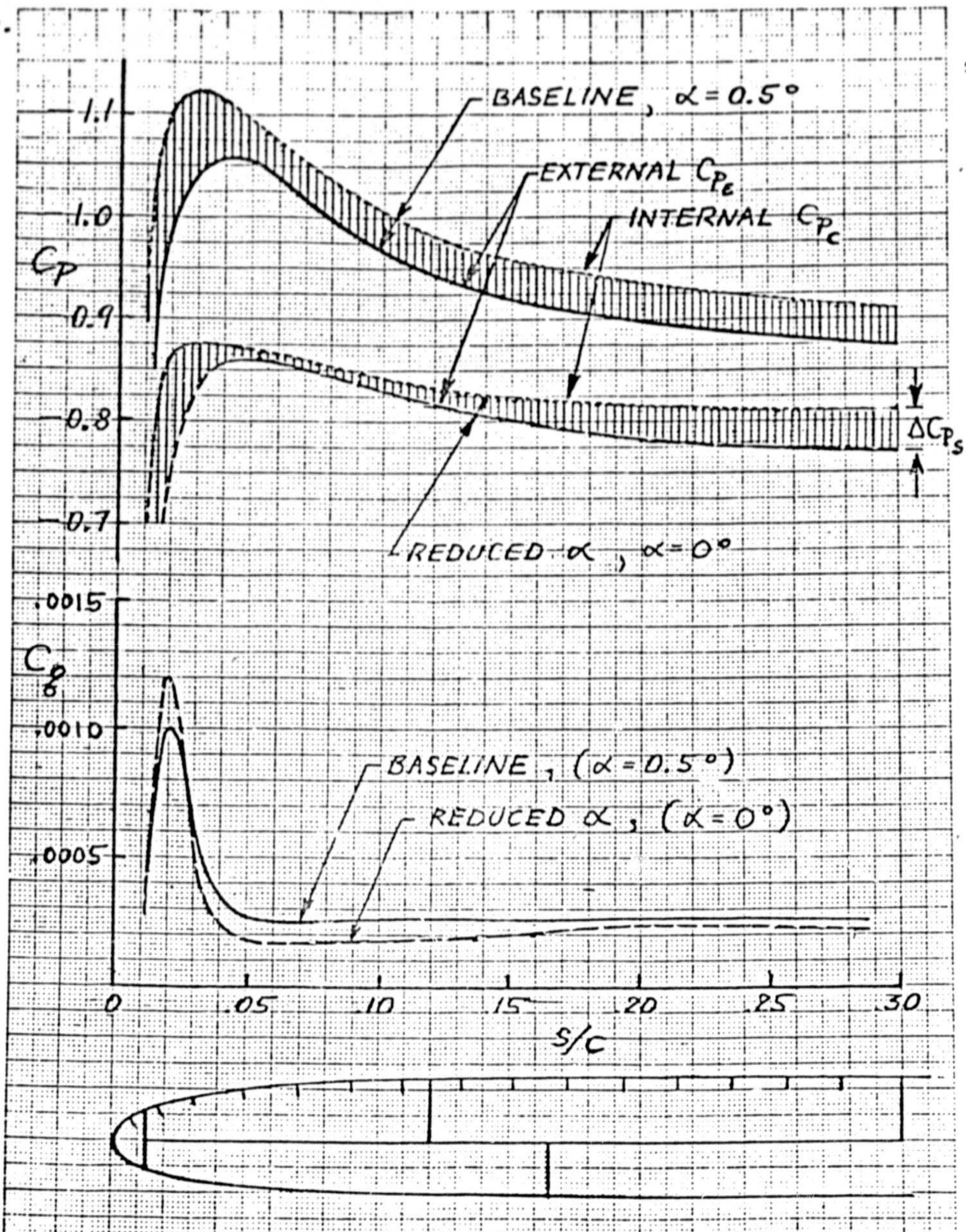

CALC		REVISED	DATE	SUCTION FLOW CHARACTERISTICS AT REDUCED INCIDENCE	
CHECK					
APR					
APR				THE BOEING COMPANY	PAGE FIG. 13